

Article

Cholesterol Significantly Affects the Interactions between Pirfenidone and DPPC Liposomes: Spectroscopic Studies

Irina M. Le-Deygen ^{*}, Anastasia S. Safronova , Polina V. Mamaeva, Anna A. Skuredina 
and Elena V. Kudryashova

Chemistry Department, Lomonosov Moscow State University, 119991 Moscow, Russia; milarika09@mail.ru (A.S.S.); mamaevapolina@yahoo.com (P.V.M.); anna.skuredina@yandex.ru (A.A.S.); helenakoudriachova@yandex.ru (E.V.K.)

* Correspondence: i.m.deygen@gmail.com; Tel.: +7-(495)939-34-34

Abstract: In this work, we studied the effect of as on the interaction of membrane DPPC with the key antifibrotic drug pirfenidone. Liposomal forms of pirfenidone were obtained using passive loading. The addition of cholesterol reduces the loading efficiency of pirfenidone by 10%. The main binding site of pirfenidone in DPPC liposomes is the carbonyl group: the interaction with PF significantly increases the proportion of low-hydrated carbonyl groups as revealed by ATR-FTIR spectroscopy. The phosphate group acts as an additional binding site; however, due to shielding by the choline group, this interaction is weak. The hydrophobic part of the bilayer is not involved in PF binding at room temperature. Cholesterol changes the way of interaction between carbonyl groups and pirfenidone probably because of the formation of two subpopulations of DPPC and causes a dramatic redistribution of carbonyl groups onto the degrees of hydration. The proportion of moderately hydrated carbonyl groups increases, apparently due to the deepening of pirfenidone into the circumpolar region of the bilayer. For the first time, a change in the microenvironment of pirfenidone upon binding to liposomes was shown: aromatic moiety interacts with the bilayer.

Keywords: liposomes; drug delivery; pirfenidone; lung fibrosis; ATR-FTIR spectroscopy



Citation: Le-Deygen, I.M.; Safronova, A.S.; Mamaeva, P.V.; Skuredina, A.A.; Kudryashova, E.V. Cholesterol Significantly Affects the Interactions between Pirfenidone and DPPC Liposomes: Spectroscopic Studies. *Biophysica* **2022**, *2*, 79–88. <https://doi.org/10.3390/biophysica2010008>

Academic Editors: Ricardo L. Mancera, Paul C Whitford and Chandra Kothapalli

Received: 24 December 2021

Accepted: 14 February 2022

Published: 16 February 2022

Publisher's Note: MDPI stays neutral with regard to jurisdictional claims in published maps and institutional affiliations.



Copyright: © 2022 by the authors. Licensee MDPI, Basel, Switzerland. This article is an open access article distributed under the terms and conditions of the Creative Commons Attribution (CC BY) license (<https://creativecommons.org/licenses/by/4.0/>).

1. Introduction

Today, all over the world, there is an urgent task of developing new drugs for rehabilitation after COVID-19. The incidence is constantly growing, new strains of the virus appear, causing not only a severe course of the disease but also a pronounced post-COVID syndrome [1,2]. One of the manifestations of this syndrome is the development of pulmonary fibrosis [3,4], which is similar in its properties to idiopathic pulmonary fibrosis (IPF). According to Dr Christine Kim Garcia [5], 20% of non-mechanically ventilated survivors of severe COVID-19, and 72% of mechanically ventilated individuals had fibrotic-like radiographic abnormalities 4 months after hospitalization.

For the treatment of idiopathic pulmonary fibrosis, the FDA has approved two drugs, pirfenidone (PF) and nintedanib [6,7], which are effective in IPF correction. According to the latest data, pirfenidone is also capable of being active in the correction of post-COVID pulmonary fibrosis, which opens up new horizons for the use of this drug around the world. In India, some clinical trials are already being conducted (e.g., CTRI/2021/09/036442).

For the massive use of pirfenidone in the rehabilitation of patients with post-COVID pulmonary fibrosis and IPF, a simple and convenient dosage form is needed, which would not require a hospital stay and at the same time ensure high efficiency of therapy, including high bioavailability in the target lung tissues. Such a dosage form can be an inhaled liposomal form of pirfenidone, including one based on dipalmitoylphosphatidylcholine (DPPC), a major phospholipid of human lung surfactant [8]. Inhaled forms of PF prevent the development of phototoxicity [9,10].

Liposomes represent promising delivery systems for a variety of drugs, and many liposomal forms are available on the market and have proven themselves in medical practice, e.g., Doxil. Inhaled liposomal drugs are successful: Arikace[®] (liposomal amikacin) [11] and Pulmaquin[®] (liposomal ciprofloxacin). Liposomal inhaled forms of pirfenidone with variable data have been already described in the literature [12]. Liposomal forms of pirfenidone provide more beneficial biodistribution cause fewer side effects; however, there is currently a lack of data on the physicochemical process of interaction of pirfenidone with the bilayer.

However, despite the high clinical potential, the liposomal PF mechanism of interaction between PF and the lipid matrix is still unclear. The composition of the lipid matrix has a key effect on the nature of the interaction of the bilayer with the drug, as demonstrated in classic papers with doxorubicin [13] and amphotericin B [14]. The authors of the review [15] found that the composition of liposomes affects incorporation efficiency, stability, the surface charge of the liposomal formulation of the drug, pharmacokinetics, pharmacodynamics and biodistribution of the active substance.

On the other hand, it's well-known that alveolar epithelial Type-II cells synthesize saturated phosphatidylcholine, which, together with cholesterol, exist in lamellar bodies [16]. Thus, the composition of liposomes affects not only the nature of the interaction of the bilayer with the drug but also affects the affinity of the drug delivery system for target tissues. The presence of cholesterol in the composition of the liposomal form of pirfenidone has the potential to increase the effectiveness of therapy. Thus, for the further development of effective pharmaceutical formulations of pirfenidone based on liposomes, it is necessary to comprehensively study the nature of its interaction with liposomes of various lipid compositions [17]. The inclusion of 10% cholesterol in the DPPC matrix is a classic approach to producing a liposomal drug formulation [18]; at such a concentration, it is possible to detect interesting effects of the influence of the composition of liposomes on the interaction with various ligands; however, the proportion of cholesterol is not yet so high as to dramatically change the properties of the bilayer.

Among all methods for studying the mechanisms of drug interaction with liposomes, ATR-FTIR spectroscopy attracts special attention. This method provides unique information about the microenvironment of the functional groups of biomolecules [19], which allows one to study in detail the nature of the interaction of drugs with the bilayer.

In our work, we set the goal of studying the effect of the composition of the lipid matrix on the nature of the interaction of liposomes with pirfenidone using sophisticated spectral methods, primarily ATR-FTIR spectroscopy.

2. Materials and Methods

2.1. Materials

Pirfenidone was obtained from Sigma Aldrich, St. Louis, MO, USA; DPPC, cholesterol Avanti Polar Lipids, Alabaster, AL, USA. Sodium phosphate buffer tablets for solution preparation Pan-Eco, Russia

2.2. Liposome Preparation

A solution of lipids in chloroform was taken in the desired ratio (DPPC or DPPC: Cholesterol 90:10). CHCl₃ solvent was carefully removed on a vacuum rotary evaporator at a temperature not exceeding 55 °C. The resulting thin film of lipids was dispersed in 0.02 M sodium phosphate buffer, pH 7.4.

The suspension was exposed to an ultrasonic bath (37 Hz) for 5 min. Next, the suspension was sonicated (22 kHz) for 600 s (2 × 300 s) in a continuous mode with constant cooling on a 4710 "Cole-Parmer Instrument" disperser.

2.3. Liposomal Form of Pirfenidone Preparation

To obtain pirfenidone-loaded liposomes by passive loading, the previously described method was used [20]. The lipid film was dispersed with 0.01 M sodium phosphate-

buffered solution, pH 7.4, containing pirfenidone (2 mg/mL). The resulting suspension was exposed to an ultrasonic bath (37 Hz) for 5 min; then it was treated with ultrasound (22 kHz) for 600 s (2×300 s) in continuous mode with constant cooling on a 4710 “Cole-Parmer Instrument” disperser (Vernon Hills, IL, USA). Free PF was separated by dialysis against sodium phosphate-buffered saline (Serva, Heidelberg, Germany; MW cut-off 3500) for 2 h, followed by determination of the degree of PF incorporation into the vesicles.

2.4. DLS Measurements

Determination of the size and zeta-potential of vesicles was carried out using a Zetasizer Nano S Malvern (Malvern Panalytical Ltd, Malvern, UK) (4 mW He–Ne laser, 633 nm) in a thermostated cell at 22 °C. Malvern software was used.

2.5. UV-Vis Spectroscopy

UV spectra of PF were recorded on a UV-visible spectrometer AmerSharm Biosciences UltraSpec 2100 pro (Holliston, MA, USA) in the range from 200 to 400 nm in a 1 mL quartz cuvette Hellma Analytics (Müllheim, Germany). The main characteristic peak of PF was observed at 310 nm.

2.6. ATR-FTIR Spectroscopy

The spectra were recorded using a Tensor 27 IR Fourier spectrometer (Bruker, Germany) equipped with an MCT detector cooled with liquid nitrogen and a thermostat (Huber, Raleigh, NC, USA). The measurements were carried out in a BioATR II thermostated cell (Bruker, Germany) using a single reflection ZnSe element at 22 °C and continuous purging of the system with dry air using a compressor (Redditch, UK). An aliquot (50 μ L) of the corresponding solution was applied to the internal reflection element. The spectrum was recorded three times in the range from 4000 to 950 cm^{-1} with a resolution of 1 cm^{-1} ; performed 70-fold, scanning and averaging. The background was registered in the same way and was automatically subtracted by the program. The spectra were analyzed using the Opus 7.0 software, Bruker. When recording the ATR-FTIR spectra of liposomes loaded with PF, a solution of PF in equal concentration was used as a background solution. When recording the ATR-FTIR spectra of PF in liposomes, spectra of the corresponding unloaded liposomes were subtracted as a background solution.

Carbonyl groups spectral region deconvolution was conducted as described [21,22]. Curve-fitting was performed using the Bruker Opus 7.5 software. The center positions of the band components were found by the second-derivative production. Bands were fitted by components of Gauss shape, with a correlation of at least 0.995. For DPPC liposomes, two components were observed: 1730 cm^{-1} and 1742 cm^{-1} . For empty DPPC:Cholesterol liposomes model included components 1718 cm^{-1} , 1729 cm^{-1} , 1741 cm^{-1} and for PF-loaded liposomes model included components 1718 cm^{-1} , 1729 cm^{-1} , 1736 cm^{-1} , 1741 cm^{-1} and 1751 cm^{-1} .

3. Results

3.1. Pirfenidone Characterization

To study the interaction of pirfenidone with liposomes, we checked preliminary experiments on PF characterization. In the UV spectrum of PF, there is a characteristic absorption peak of 310 nm, which is well suited for determining the PF content in a solution in the range of concentrations up to 45 microgram/mL (Figure 1a).

While UV spectroscopy is well suited for analyzing pirfenidone content and determining liposome loading efficiency, the ATR-FTIR spectrum of PF appears to be useful for deeper analysis of the microenvironment of its functional groups (Table 1, Figures 1b and S1). Figure 1b shows the spectrum of pirfenidone, and its main absorption bands correspond to the following bond vibrations according to [23–26]. Absorption band 1663 cm^{-1} corresponds to C=O stretch vibration, while two sharp and narrow bands, 1557 cm^{-1} and

1536 cm^{-1} , correspond to aromatic oscillations. A less intensive but clear and sharp band at 1495 cm^{-1} corresponds to βHCH aromatic bond vibrations.

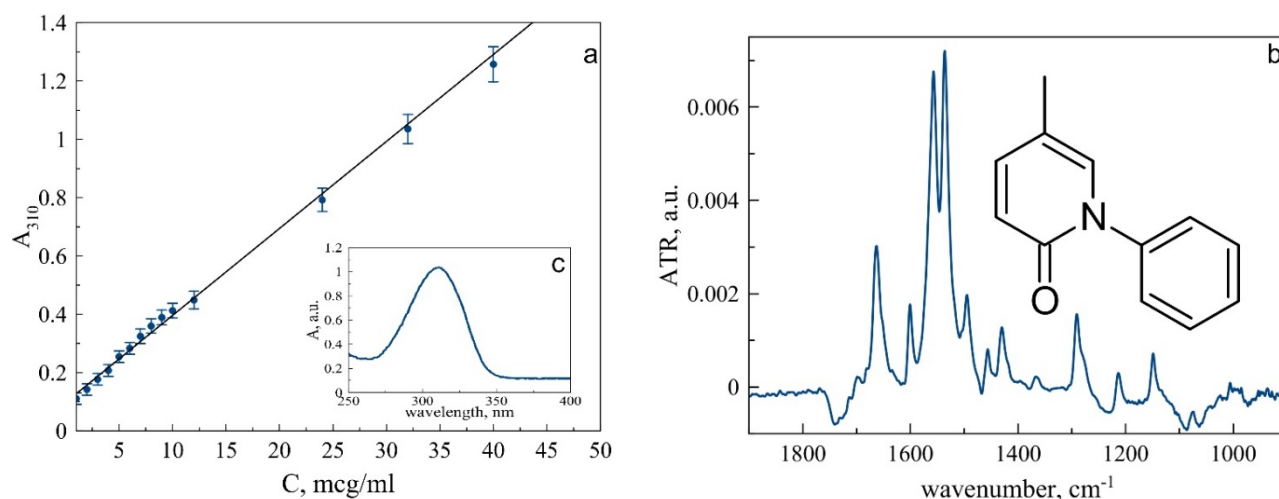


Figure 1. (a). Calibration curve for pirfenidone in sodium-phosphate-buffered solution based on UV-Vis spectra. (b). ATR-FTIR spectra of pirfenidone (4 mg/mL) in 0.02 M sodium-phosphate-buffered solution pH 7.4. In insertion: pirfenidone structure. c. UV-spectrum of pirfenidone.

Table 1. Main peak positions in ATR-FTIR spectra of pirfenidone solution and DPPC and DPPC:Chol 90:10 liposomes.

Functional Group	PF, cm^{-1}	PF DPPC, cm^{-1}	PF DPPC:Chol 90:10, cm^{-1}
C=O stretch [25]	1663	1665	1665
C=C aromatic [23,24,26]	1557	1557	1555
	1536	1536	1535
βHCH [24]	1495	1492	1490

3.2. Physico-Chemical Characterization of Liposomal Form of Pirfenidone

We set the task to study the effect of the composition of the lipid matrix on the interaction of the bilayer with pirfenidone. DPPC, a major phospholipid of human pulmonary surfactant, was selected as the main component of liposomes. It is known that the addition of cholesterol can significantly affect the properties of liposomes; therefore, in this work, liposomes based on DPPC containing 10% of mass cholesterol were studied.

Encapsulation efficiency (EE) of pirfenidone was determined by analyzing the washings after dialysis. As a control of the physicochemical properties of liposomes, the zeta potential and hydrodynamic radius were determined by the method of dynamic light scattering (Table 2).

Table 2. Encapsulation efficacy, ζ -potential and hydrodynamic diameter of liposomal form of pirfenidone. 0.02 M Na-phosphate-buffered solution, pH 7.4, 22 °C.

Sample	Encapsulation Efficacy, %	ζ -Potential, mV	Dh, nm
DPPC control		-10.1 ± 0.5	103 ± 2
DPPC PF	32 ± 4	-13.1 ± 0.6	107 ± 6
DPPC:Chol 90:10		-12.5 ± 0.7	100 ± 3
DPPC:Chol 90:10 PF	20 ± 3	-10.9 ± 0.5	98 ± 2

Comparing the values of zeta potentials and sizes of control liposomes and liposomal forms of PF, it should be noted that there is no reliable and significant change in these parameters when loading active molecules. The same effects we have observed for moxifloxacin, loaded into liposomes [20]. The degree of inclusion of pirfenidone in DPPC

liposomes is typical for small organic molecules: without additional measures, it does not exceed 35%. The addition of 10% cholesterol to the DPPC matrix leads to a noticeable decrease in the encapsulation efficiency, which is apparently associated with a greater membrane rigidity; however, to reveal the molecular mechanisms of drug interaction with liposomes of various compositions, a more in-depth study is required.

3.3. Mechanism of Interaction of Pirfenidone with Liposomes as Revealed by ATR-FTIR Spectroscopy

To study the molecular mechanism of the interaction of PF with the bilayer and identify the main binding sites, the main method of ATR-FTIR spectroscopy was used. This method is a highly informative spectral method suitable for studying complex colloidal systems, including liposomes [27]. This method allows a detailed study of the interaction of pirfenidone with various functional groups of lipids. The ATR-FTIR spectra of liposomes (Figure S2) contain a number of main absorption bands (Table 3), which are informative in the analysis of the interaction of liposomes with various molecules. Figure 2 show the ATR-FTIR spectrum of DPPC 100% liposomes. Symmetric and asymmetric stretching vibrations of the CH₂ group correspond to bands in the region of $2850 \pm 1 \text{ cm}^{-1}$ and $2919 \pm 1 \text{ cm}^{-1}$. These absorption bands are sensitive to changes in liposome acyl chain packing [28]. The absorption band of the carbonyl group is located in the region of $1715\text{--}1750 \text{ cm}^{-1}$ is sensitive to changes in the microenvironment on the lipid-water surface. The phosphate group of phospholipids is characterized by two stretching vibration bands: νPO_2^- s 1088 cm^{-1} and νPO_2^- as $1250\text{--}1230 \text{ cm}^{-1}$. The analytically significant νPO_2^- as band is of greatest interest as it is sensitive to the interaction of cationic ligands with the polar head of liposomes. A change in the position of absorption bands and their shape indicates a change in the microenvironment of the corresponding functional groups; thus, the analysis of ATR-FTIR spectra makes it possible to identify the main binding sites of ligands including small organic molecules [29].

Table 3. Position of the main absorption bands in the ATR-FTIR spectra of liposomes of various lipid compositions. 0.02 M sodium phosphate-buffered solution, pH 7.4, 22 °C. Error in determining the maximum of the absorption band— 1 cm^{-1} .

Sample	νCH_2 as, cm^{-1}	νCH_2 s, cm^{-1}	νCO , cm^{-1}	νPO_2^- as, cm^{-1}
DPPC control	2918	2850	1737	1223
DPPC PF	2918	2850	1736	1223, 1243 shoulder
DPPC:Chol 90:10	2918	2850	1738	1224
DPPC:Chol 90:10 PF	2918	2850	1740	1223, 1243 shoulder

When the liposomal membrane interacts with pirfenidone, the following regularities are observed. The absorption bands of CH₂ groups do not undergo significant changes, which indicates that the packing density of hydrophobic chains in the bilayer remains unchanged when pirfenidone is included in liposomes.

For the liposomal form of PF DPPC 100% and DPPC:Cholesterol 90:10, uniform changes are characteristic only in the region of absorption of the phosphate group. The appearance of a peak at 1243 cm^{-1} (Figure S3) is characteristic of a decrease in the degree of hydration of some of the phosphate groups of DPPC [28], apparently due to the formation of hydrogen bonds with pirfenidone. The uniformity of changes in the area of absorption of phosphate groups is expected because cholesterol in the bilayer is located in the hydrophobic part [30], partially interacting with the lipid–water interface. Thus, pirfenidone binds to the phosphate group of DPPC both in monocomponent liposomes and in cholesterol-containing ones.

It is important to study the state of lipid carbonyl groups when interacting with active molecules because they are located at the lipid-water interface [31]. Analysis of changes in the absorption range of carbonyl groups will lead to a conclusion about the interaction of drugs with the bilayer [22]. It is known that the absorption band of the carbonyl group consists of several components [31], usually associated with high, medium

and low hydrated carbonyl groups [22]. The higher the degree of hydration of the carbonyl group, the lower is the characteristic wavenumber of the corresponding component. The position and number of components depend on the composition of the liposomes [31,32]. The ratio of the integral fractions of the components is associated with the redistribution of carbonyl groups according to the degrees of hydration.

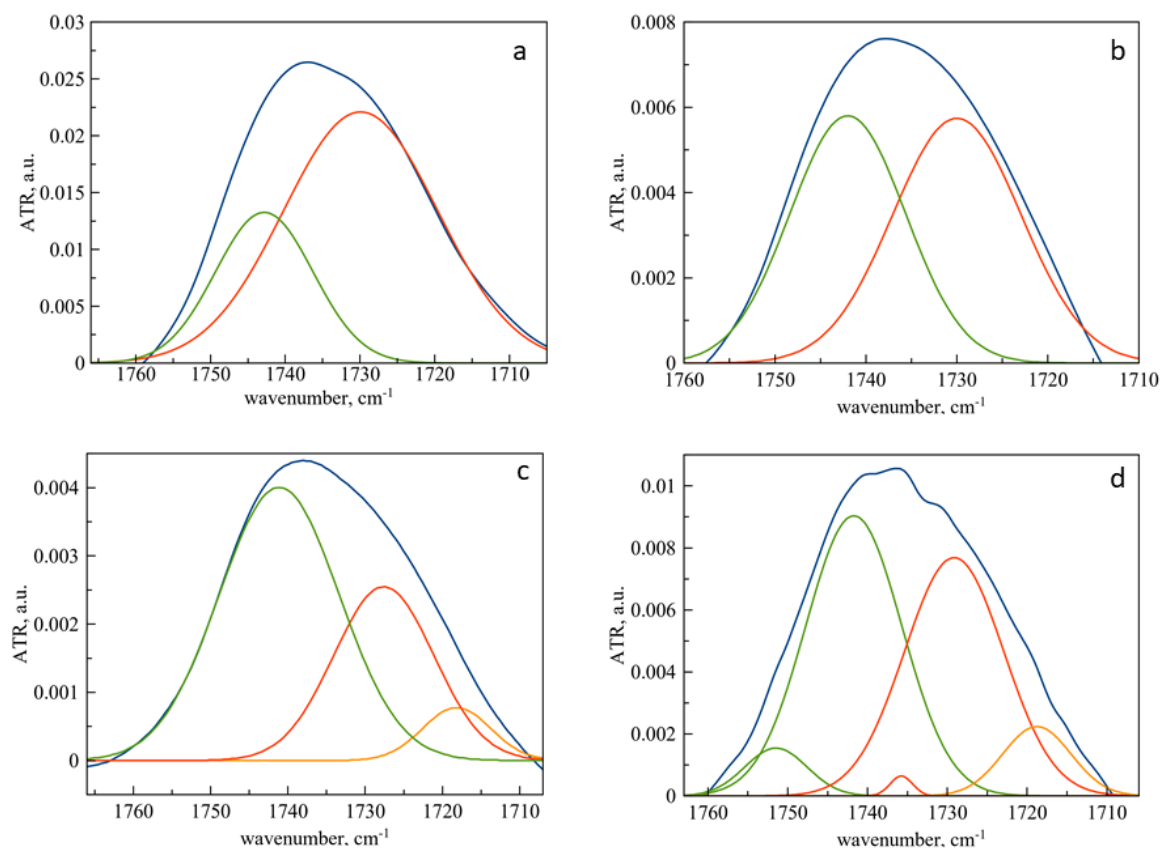


Figure 2. ATR-FTIR spectra of liposomes and liposomal forms of pirfenidone: carbonyl group area. Deconvolution was conducted with Gaussians. The blue line is the initial spectrum, green—component of low hydrated carbonyl groups, red—component of medium hydrated carbonyl groups, orange—component of high hydrated carbonyl groups. (a) DPPC liposomes. (b) DPPC liposomes, loaded with pirfenidone. (c) DPPC:Chol 90:10 liposomes. (d) DPPC:Chol 90:10 liposomes, loaded with pirfenidone. 0.02 M sodium-phosphate-buffered solution pH 7.4.

Figure 2 show the results of deconvolution of the spectra of liposomes and liposomal forms of pirfenidone. Quantitative data on the redistribution of carbonyl groups by degrees of hydration are presented in Table 4. For monocomponent DPPC liposomes, the absorption band of the carbonyl group consists of two components corresponding to the medium (1730 cm^{-1}) and low hydrated groups (1742 cm^{-1}). Moreover, the dominant form is moderately hydrated carbonyl groups [33] (1730 cm^{-1}), which corresponds to the gel-like state of the DPPC membrane [34].

Table 4. Integral share of carbonyl groups components. 0.02 M sodium phosphate-buffered solution, pH 7.4, 22 °C. SD ($n = 3$) 5%.

Sample	Low Hydrated, %	Medium Hydrated, %	High Hydrated
DPPC control	27	73	-
DPPC PF	48	52	-
DPPC:Chol 90:10	61	32	7
DPPC:Chol 90:10 PF	51	41	8

The inclusion of pirfenidone leads to a redistribution of carbonyl groups according to the degrees of hydration: the proportion of low-hydrated groups doubles. This phenomenon corresponds to the destruction of hydrogen bonds between carbonyl groups and water molecules due to the formation of new bonds with pirfenidone molecules. A significant increase in the integral share of low-hydrated carbonyl groups (Figure 2b) indicates a possible interaction of pirfenidone with the circumpolar region of the bilayer.

Thus, the interaction of DPPC liposomes with pirfenidone has the following characteristics. The main binding site is the carbonyl group: the interaction with PF significantly increases the ratio of low-hydrated carbonyl groups. The phosphate group acts as an additional binding site; however, due to shielding by the choline group, this interaction is weak. The hydrophobic part of the bilayer is not involved in PF binding at room temperature.

In the case of two-component liposomes containing 10% cholesterol, the absorption band of the carbonyl group contains at least three components (Figure 2c). The complication of the spectral pattern is expected since the introduction of even a small amount of cholesterol significantly affects the physicochemical properties of the bilayer and is reflected in the fine structure of the ATR-FTIR spectrum. It is known that cholesterol in mixtures with saturated lipids increases membrane permeability lowers the gel-liquid crystal phase transition temperature and determines the physicochemical properties of the liposome [30,35,36]. Unlike DPPC liposomes, vesicles containing cholesterol are more rigid, and this explains the predominance of low-hydrated carbonyl groups.

The incorporation of pirfenidone into liposomes containing cholesterol leads to a dramatic redistribution of carbonyl groups onto the degrees of hydration (Figure 2d). The proportion of moderately hydrated carbonyl groups increases, apparently due to the deepening of pirfenidone into the circumpolar region of the bilayer.

Thus, membrane rigidity plays a significant role in the nature of the interaction of liposomes with pirfenidone, and the carbonyl group of lipids is an important binding site for an active molecule.

3.4. Changes in the Microenvironment of Pirfenidone upon Loading into Liposomes as Revealed by ATR-FTIR Spectroscopy

As mentioned in Section 3.1, a number of informative absorption bands are present in the ATR-FTIR spectrum of pirfenidone. When an active molecule is loaded into liposomes, some absorption bands are displaced, which indicates a change in the microenvironment of some functional groups of pirfenidone (Table 1, Figure S1).

Absorption band 1663 cm^{-1} corresponding to γOC in heterocycle + γCC aromatic bonds shifts to 1665 cm^{-1} , indicating an interaction of aromatic moiety of PF with the bilayer. This result is expected since the aromatic moiety contains both a carbonyl group and a nitrogen atom in the heterocycle.

Analyzing the displacements of the remaining absorption bands, uniform changes should be noted, while for cholesterol-containing liposomes, they are more pronounced. This is clearly manifested for the band at 1495 cm^{-1} , which shifts up to 1490 cm^{-1} in the case of cholesterol-containing liposomes. Probably, when pirfenidone is anchored into the bilayer, the vibrations βHCH become more difficult; however, this requires a separate study in the future.

4. Conclusions

In this work, we studied the effect of cholesterol on the interaction of membrane DPPC with the key antifibrotic drug pirfenidone. Liposomal forms of pirfenidone were obtained via passive loading, and the loading efficiency depends on the membrane rigidity: the addition of cholesterol reduces the loading efficiency. The main binding sites were established: the carbonyl and phosphate groups of DPPC. At the same time, for the first time, using the deconvolution of bands in the ATR-FTIR spectrum of liposomes, the redistribution of carbonyl groups according to the degrees of hydration was demonstrated when interacting with pirfenidone.

Cholesterol significantly affects the interaction of PF with the membrane. Since pirfenidone is unable to penetrate into the bilayer at room temperature, the main interaction occurs at the lipid-water interface. In the case of monocomponent liposomes, interaction with an active molecule leads to a decrease in the degree of hydration of carbonyl groups, apparently due to the formation of hydrogen bonds with PF. A more rigid cholesterol-containing membrane is characterized by a more complex pattern of distribution of carbonyl groups by degrees of hydration. This is probably due to the existence of at least two populations of DPPC molecules: “sandwiched” between cholesterol molecules and free ones, as was established by the method of computer simulation [30]. These two subpopulations appear to interact differently with pirfenidone.

It was found that the anchoring of pirfenidone in the bilayer is accompanied by a shift of the main bands in the spectrum of the active molecule, which indicates a change in the microenvironment of both the heterocycle and the benzene ring. The structure of the most active molecule plays a decisive role in the nature of the interaction with the bilayer. Previously, we have found [20] that moxifloxacin is capable of anchoring in the bilayer and actively interacts primarily with the phosphate groups of lipids due to the sterically free nitrogen atom in the heterocyclic fragment, then pirfenidone preferentially binds to carbonyl groups, significantly increasing the proportion of low-hydrated groups in the DPPC membrane.

Obtained data serve as the basis for discovering the mechanism of interaction between pirfenidone and biomembranes.

Supplementary Materials: The following are available online at <https://www.mdpi.com/article/10.3390/biophysica2010008/s1>, Figure S1: Normalized ATR-FTIR spectra of pirfenidone (blue) and liposomal forms of pirfenidone. Main bands of pirfenidone are presented. 0.02 M sodium-phosphate buffer solution, pH 7.4, 22 °C. Figure S2: ATR-FTIR spectrum of DPPC liposomes. Total lipid concentration 5 mg/mL. 0.02 M sodium-phosphate buffer solution, pH 7.4, 22 °C. Figure S3: Normalized ATR-FTIR spectrum of DPPC liposomes and liposomal forms of pirfenidone in the area of asymmetric valence oscillation of phosphate groups. Total lipid concentration 5 mg/mL. 0.02 M sodium-phosphate buffer solution, pH 7.4, 22 °C.

Author Contributions: Conceptualization, I.M.L.-D., E.V.K. and A.A.S.; methodology, data curation A.S.S., P.V.M. and I.M.L.-D.; original draft preparation, E.V.K. and A.A.S.; writing—review and editing. All authors have read and agreed to the published version of the manuscript.

Funding: The research was funded by RFBR and Moscow city Government, project number 21-33-70035.

Conflicts of Interest: The authors declare no conflict of interest. The funders had no role in the design of the study; in the collection, analyses, or interpretation of data; in the writing of the manuscript, or in the decision to publish the results.

References

1. Oronsky, B.; Larson, C.; Hammond, T.C.; Oronsky, A.; Kesari, S.; Lybeck, M.; Reid, T.R. A Review of Persistent Post-COVID Syndrome (PPCS). *Clin. Rev. Allergy Immunol.* **2021**, 1–9. [[CrossRef](#)] [[PubMed](#)]
2. Maltezou, H.; Pavli, A.; Tsakris, A. Post-COVID Syndrome: An Insight on Its Pathogenesis. *Vaccines* **2021**, *9*, 497. [[CrossRef](#)] [[PubMed](#)]
3. Udawadia, Z.; Koul, P.; Richeldi, L. Post-COVID lung fibrosis: The tsunami that will follow the earthquake. *Lung India* **2021**, *38*, S41–S47. [[CrossRef](#)] [[PubMed](#)]
4. Scelfo, C.; Fontana, M.; Casalini, E.; Menzella, F.; Piro, R.; Zerbini, A.; Spaggiari, L.; Ghidorsi, L.; Ghidoni, G.; Facciolongo, N.C. A Dangerous Consequence of the Recent Pandemic: Early Lung Fibrosis Following COVID-19 Pneumonia—Case Reports. *Ther. Clin. Risk Manag.* **2020**, *16*, 1039–1046. [[CrossRef](#)] [[PubMed](#)]
5. McGroder, C.F.; Zhang, D.; Choudhury, M.A.; Salvatore, M.M.; D’Souza, B.M.; Hoffman, E.A.; Wei, Y.; Baldwin, M.R.; Garcia, C.K. Pulmonary fibrosis 4 months after COVID-19 is associated with severity of illness and blood leucocyte telomere length. *Thorax* **2021**, *76*, 1242–1245. [[CrossRef](#)]
6. Hughes, G.; Toellner, H.; Morris, H.; Leonard, C.; Chaudhuri, N. Real World Experiences: Pirfenidone and Nintedanib are Effective and Well Tolerated Treatments for Idiopathic Pulmonary Fibrosis. *J. Clin. Med.* **2016**, *5*, 78. [[CrossRef](#)]

7. Richeldi, L.; Du Bois, R.M.; Raghu, G.; Azuma, A.; Brown, K.K.; Costabel, U.; Cottin, V.; Flaherty, K.R.; Hansell, D.M.; Inoue, Y.; et al. Efficacy and Safety of Nintedanib in Idiopathic Pulmonary Fibrosis. *N. Engl. J. Med.* **2014**, *370*, 2071–2082. [[CrossRef](#)]
8. Nkadi, P.O.; Merritt, T.A.; Pillers, D.-A.M. An overview of pulmonary surfactant in the neonate: Genetics, metabolism, and the role of surfactant in health and disease. *Mol. Genet. Metab.* **2009**, *97*, 95–101. [[CrossRef](#)]
9. Onoue, S.; Seto, Y.; Kato, M.; Aoki, Y.; Kojo, Y.; Yamada, S. Inhalable Powder Formulation of Pirfenidone with Reduced Phototoxic Risk for Treatment of Pulmonary Fibrosis. *Pharm. Res.* **2013**, *30*, 1586–1596. [[CrossRef](#)]
10. Kaminskis, L.M.; Landersdorfer, C.B.; Bischof, R.J.; Leong, N.; Ibrahim, J.; Davies, A.N.; Pham, S.; Beck, S.; Montgomery, A.B.; Surber, M.W. Aerosol Pirfenidone Pharmacokinetics after Inhaled Delivery in Sheep: A Viable Approach to Treating Idiopathic Pulmonary Fibrosis. *Pharm. Res.* **2019**, *37*, 3. [[CrossRef](#)]
11. Clancy, J.P.; Dupont, L.; Konstan, M.W.; Billings, J.; Fustik, S.; Goss, C.H.; Lymp, J.; Minic, P.; Quittner, A.L.; Rubenstein, R.C.; et al. Phase II studies of nebulised Arikace in CF patients with *Pseudomonas aeruginosa* infection. *Thorax* **2013**, *68*, 818–825. [[CrossRef](#)] [[PubMed](#)]
12. Parvathaneni, V.; Kulkarni, N.S.; Shukla, S.K.; Farrales, P.T.; Kunda, N.K.; Muth, A.; Gupta, V. Systematic Development and Optimization of Inhalable Pirfenidone Liposomes for Non-Small Cell Lung Cancer Treatment. *Pharmaceutics* **2020**, *12*, 206. [[CrossRef](#)] [[PubMed](#)]
13. Mayer, L.D.; Tai, L.C.; Ko, S.C.; Masin, D.; Ginsberg, R.S.; Cullis, P.R.; Bally, M.B. Influence of Vesicle Size, Lipid Composition, and Drug-to-Lipid Ratio on the Biological Activity of Liposomal Doxorubicin in Mice. *Cancer Res.* **1989**, *49*, 5922–5930. [[PubMed](#)]
14. Szoka, F.C.; Milholland, D.; Barza, M. Effect of lipid composition and liposome size on toxicity and in vitro fungicidal activity of liposome-intercalated amphotericin B. *Antimicrob. Agents Chemother.* **1987**, *31*, 421–429. [[CrossRef](#)] [[PubMed](#)]
15. Large, D.E.; Abdelmessih, R.G.; Fink, E.A.; Auguste, D.T. Liposome composition in drug delivery design, synthesis, characterization, and clinical application. *Adv. Drug Deliv. Rev.* **2021**, *176*, 113851. [[CrossRef](#)]
16. Kellaway, I.W.; Farr, S.J. Liposomes as drug delivery systems to the lung. *Adv. Drug Deliv. Rev.* **1990**, *5*, 149–161. [[CrossRef](#)]
17. Andrade, S.; Ramalho, M.J.; Loureiro, J.A.; Pereira, M.C. Liposomes as biomembrane models: Biophysical techniques for drug-membrane interaction studies. *J. Mol. Liq.* **2021**, *334*, 116141. [[CrossRef](#)]
18. Efimova, A.A.; Trosheva, K.S.; Krasnikov, E.A.; Krivtsov, G.G.; Yaroslavov, A.A. Complexes of Anionic Cholesterol-Containing Liposomes and Cationic Chitosan Microparticles. *Polym. Sci. Ser. A* **2019**, *61*, 737–742. [[CrossRef](#)]
19. Stuart, B. FTIR of Biomolecules. In *Encyclopedia of Molecular Cell Biology and Molecular Medicine*; Wiley-Blackwell: Hoboken, NJ, USA, 2006; pp. 651–683. [[CrossRef](#)]
20. Le-Deygen, I.M.; Skuredina, A.A.; Safronova, A.S.; Yakimov, I.D.; Kolmogorov, I.M.; Deygen, D.M.; Burova, T.V.; Grinberg, N.V.; Grinberg, V.Y.; Kudryashova, E.V. Moxifloxacin interacts with lipid bilayer, causing dramatic changes in its structure and phase transitions. *Chem. Phys. Lipids* **2020**, *228*, 104891. [[CrossRef](#)]
21. Deygen, I.M.; Seidl, C.; Kölmel, D.K.; Bednarek, C.; Heissler, S.; Kudryashova, E.V.; Bräse, S.; Schepers, U. Novel Prodrug of Doxorubicin Modified by Stearoylspermine Encapsulated into PEG-Chitosan-Stabilized Liposomes. *Langmuir* **2016**, *32*, 10861–10869. [[CrossRef](#)]
22. Deygen, I.; Kudryashova, E.V. Structure and stability of anionic liposomes complexes with PEG-chitosan branched copolymer. *Russ. J. Bioorg. Chem.* **2014**, *40*, 547–557. [[CrossRef](#)]
23. Soni, S.R.; Bhunia, B.K.; Kumari, N.; Dan, S.; Mukherjee, S.; Mandal, B.B.; Ghosh, A. Therapeutically Effective Controlled Release Formulation of Pirfenidone from Nontoxic Biocompatible Carboxymethyl Pullulan-Poly(vinyl alcohol) Interpenetrating Polymer Networks. *ACS Omega* **2018**, *3*, 11993–12009. [[CrossRef](#)] [[PubMed](#)]
24. Manjusha, P.; Prasana, J.C.; Muthu, S.; Raajaraman, B. Density functional studies and spectroscopic analysis (FT-IR, FT-Raman, UV-visible, and NMR) with molecular docking approach on an antifibrotic drug Pirfenidone. *J. Mol. Struct.* **2020**, *1203*, 127394. [[CrossRef](#)]
25. Abnoos, M.; Mohseni, M.; Mousavi, S.A.J.; Ashtari, K.; Ilka, R.; Mehravi, B. Chitosan-alginate nano-carrier for transdermal delivery of pirfenidone in idiopathic pulmonary fibrosis. *Int. J. Biol. Macromol.* **2018**, *118*, 1319–1325. [[CrossRef](#)] [[PubMed](#)]
26. Pardeshi, S.; Patil, P.; Rajput, R.; Mujumdar, A.; Naik, J. Preparation and characterization of sustained release pirfenidone loaded microparticles for pulmonary drug delivery: Spray drying approach. *Dry. Technol.* **2021**, *39*, 337–347. [[CrossRef](#)]
27. Bensikaddour, H.; Snoussi, K.; Lins, L.; Van Bambeke, F.; Tulkens, P.M.; Brasseur, R.; Goormaghtigh, E.; Mingeot-Leclercq, M.-P. Interactions of ciprofloxacin with DPPC and DPPG: Fluorescence anisotropy, ATR-FTIR and ³¹P NMR spectroscopies and conformational analysis. *Biochim. Biophys. Acta (BBA)-Biomembr.* **2008**, *1778*, 2535–2543. [[CrossRef](#)] [[PubMed](#)]
28. Manrique-Moreno, M.; Garidel, P.; Suwalsky, M.; Howe, J.; Brandenburg, K. The membrane-activity of Ibuprofen, Diclofenac, and Naproxen: A physico-chemical study with lecithin phospholipids. *Biochim. Biophys. Acta (BBA)-Biomembr.* **2009**, *1788*, 1296–1303. [[CrossRef](#)]
29. Tretiakova, D.; Le-Deigen, I.; Onishchenko, N.; Kuntsche, J.; Kudryashova, E.; Vodovozova, E. Phosphatidylinositol Stabilizes Fluid-Phase Liposomes Loaded with a Melphalan Lipophilic Prodrug. *Pharmaceutics* **2021**, *13*, 473. [[CrossRef](#)]
30. Sugár, I.P.; Chong, P.L.-G. A Statistical Mechanical Model of Cholesterol/Phospholipid Mixtures: Linking Condensed Complexes, Superlattices, and the Phase Diagram. *J. Am. Chem. Soc.* **2011**, *134*, 1164–1171. [[CrossRef](#)]
31. Disalvo, E.A.; Frias, M.A. Water State and Carbonyl Distribution Populations in Confined Regions of Lipid Bilayers Observed by FTIR Spectroscopy. *Langmuir* **2013**, *29*, 6969–6974. [[CrossRef](#)]

32. Arsov, Z.; Quaroni, L. Direct interaction between cholesterol and phosphatidylcholines in hydrated membranes revealed by ATR-FTIR spectroscopy. *Chem. Phys. Lipids* **2007**, *150*, 35–48. [[CrossRef](#)] [[PubMed](#)]
33. Vernooij, E.A.A.M.; Bosch, J.J.K.-V.D.; Crommelin, D.J.A. Fourier Transform Infrared Spectroscopic Determination of the Hydrolysis of Poly(ethylene glycol)—Phosphatidylethanolamine-Containing Liposomes. *Langmuir* **2002**, *18*, 3466–3470. [[CrossRef](#)]
34. Wei, T.-T.; Sun, H.-Y.; Deng, G.; Gu, J.-Y.; Guo, H.-Y.; Xu, J.; Wu, R.-G. The interaction of paeonol with DPPC liposomes. *J. Therm. Anal.* **2018**, *132*, 685–692. [[CrossRef](#)]
35. Beck, Z.; Matyas, G.R.; Alving, C.R. Detection of liposomal cholesterol and monophosphoryl lipid A by QS-21 saponin and *Limulus polyphemus* amoebocyte lysate. *Biochim. Biophys. Acta (BBA)-Biomembr.* **2015**, *1848*, 775–780. [[CrossRef](#)]
36. Briuglia, M.-L.; Rotella, C.M.; McFarlane, A.; Lamprou, D.A. Influence of cholesterol on liposome stability and on in vitro drug release. *Drug Deliv. Transl. Res.* **2015**, *5*, 231–242. [[CrossRef](#)]